Article

Investigating the Effect of Fine Particulate Matter (PM$_{2.5}$) Emission Reduction on Surface-Level Ozone (O$_3$) during Summer across the UK

Lydia Curley [1], Rayne Holland [1], M. Anwar H. Khan [1] and Dudley E. Shallcross [1,2,*]

[1] School of Chemistry, University of Bristol, Cantock's Close, Bristol BS8 1TS, UK;
lydiacurley01@gmail.com (L.C.); rayne.holland@bristol.ac.uk (R.H.); anwar.khan@bristol.ac.uk (M.A.H.K.)

[2] Department of Chemistry, University of the Western Cape, Robert Sobukwe Road, Bellville 7305, South Africa

* Correspondence: d.e.shallcross@bristol.ac.uk

Abstract: UK air pollutant data collected over a 10-year period (2010–2019) from 46 sites with Urban Traffic, Urban Background, Suburban Background, Rural Background, and Urban Industrial environmental types were analysed to study the relationships between [NO] vs. [PM$_{2.5}$] and [O$_3$] vs. [PM$_{2.5}$] during the summer for each site type. These results were used to describe the consequence of recent PM$_{2.5}$ reductions on NO and O$_3$ concentrations at different site types across the UK. The strongest positive [NO] vs. [PM$_{2.5}$] correlation was observed for the Urban Traffic site type overall, but it displayed the weakest positive [O$_3$] vs. [PM$_{2.5}$] correlation. Analysis of individual Urban Traffic sites revealed an overall negative [O$_3$] vs. [PM$_{2.5}$] gradient at the London Marylebone Road (LMR) site. A sharp 35% PM$_{2.5}$ decrease occurred at LMR between 2011 and 2015 before annual mean concentrations plateaued. Further examination of annual correlations revealed negative [O$_3$] vs. [PM$_{2.5}$] gradients in each year directly proceeding the sharp 35% PM$_{2.5}$ decrease at LMR. NO$_x$ fluctuations were minimal and accompanied by comparable volatile organic compound (VOC) decreases; thus, VOC-limited chemistry at LMR was deemed to not be the primary cause of O$_3$ increases. Instead, PM$_{2.5}$ reductions are suggested to be a more significant factor in causing O$_3$ increases, as suppression of O$_3$ production by PM$_{2.5}$ chemistry decreases with declining [PM$_{2.5}$]. The remaining two Urban Traffic sites in Birmingham did not display a negative [O$_3$] vs. [PM$_{2.5}$] correlation in the years studied. This was partly ascribed to the Birmingham measurement sites not being under the influence of the street canyon effect like LMR. Principal attribution was to the lower-average absolute initial PM$_{2.5}$ concentrations and absence of a significant (>26%) continuous mean PM$_{2.5}$ decline of greater than 2 years. This study therefore proposed a threshold initial PM$_{2.5}$ concentration (*t*) above which O$_3$ suppression by PM$_{2.5}$ chemistry is sufficient to induce O$_3$ increases when average PM$_{2.5}$ concentrations significantly decline (by >26% across >2 years), where 17 µg m^{-3} < *t* < 26 µg m^{-3}. Extending this analysis to additional cities across the UK as sufficient data become available would allow refinement of the proposed threshold and improved understanding of the influence from the street canyon effect. These results inform future air pollution policies, in the UK and across the globe, in which further joint reductions of PM$_{2.5}$ and O$_3$ are crucial to achieve maximum benefits to human health.

Keywords: ozone; particulate matter; secondary PM$_{2.5}$; human health impact; VOC-limited; urban traffic site

1. Introduction

Fine particulate matter (PM$_{2.5}$) is a source of chemicals and the source-specific contributions of PM$_{2.5}$ are variable across different regions [1], seasons [2], and times [3]. Each source emits a combination of various chemical constituents that have different adverse effects on air quality, climate, and human health.

Primary $PM_{2.5}$ can originate from natural sources, such as dust storms and forest fires [4,5] and anthropogenic sources, such as fossil fuel combustion, e.g., road transport including exhaust (e.g., diesel vehicles) and non-exhaust (e.g., tyre wear, brake wear, road surface abrasion from vehicles), cigarette smoke and biomass burning [6]. Secondary $PM_{2.5}$ is produced through physical and chemical processes by the gas precursors emitted from anthropogenic and biogenic sources. The Urban Background concentrations of $PM_{2.5}$ are dominated by secondary $PM_{2.5}$, e.g., in the central and southern UK reported by DEFRA [7], in the Greater Paris region reported by Beekmann et al. [8], in Northern Italy reported by De Meij et al. [9] and Larsen et al. [10]. The formation of secondary $PM_{2.5}$ is highly uncertain and varies regionally and seasonally due to meteorological changes and other variables that affect atmospheric chemistry. Thus, knowing the mass concentration of $PM_{2.5}$ alone is insufficient in identifying contributing sources or in attributing a reduction in $PM_{2.5}$ to a particular control measure. However, the relationships of $PM_{2.5}$ with co-emitted and co-produced species can provide valuable information for understanding the sources, formation, and evolution of $PM_{2.5}$ pollution.

The key precursors that allow secondary $PM_{2.5}$ formation are sulfur dioxide (SO_2), nitrogen oxides ($NO_x = NO + NO_2$), ammonia (NH_3), and volatile organic compounds (VOCs). The secondary formation of $PM_{2.5}$ due to chemical reactions in the atmosphere generally downwind and/or some distances from the original emission source [11]. Thus, the precursors, especially VOCs emitted by multiple sources, pose further problems to the identification and quantification of individual source contributions to atmospheric concentrations of $PM_{2.5}$.

Like $PM_{2.5}$, tropospheric ozone (O_3) at surface level has been subject of significant research owing to its harmful impact on human health [12,13] and adverse effects on climate and vegetation [14,15]. Ozone's strong oxidizing properties cause damage to airway cells and lining fluids, as well as causing immune-inflammatory responses inside and outside the lungs [12]. Both short-term and long-term exposure to ozone were found to be linked with increased mortality due to respiratory and cardiovascular diseases [12,13]. Ozone has phytotoxic effects on vegetation, causing injury to plant tissue and a significant decrease in crop and timber yield [15]. Tropospheric O_3 production occurs as a result of a photochemical cycle beginning with gas-phase oxidation of VOCs, catalysed by HO_x radicals, and requiring the presence of NO_x. Evidence in the literature suggests that heterogenous reactions are an important loss process for NO_x impacting O_3 production efficiency [16]. The principal heterogenous NO_x removal mechanism is via the hydrolysis of N_2O_5 which is much slower in the gas phase. Field observations and laboratory studies support the efficient uptake of N_2O_5 [17,18], with said studies measuring the reaction probability (γ) to be in the range of 0.01–1 for aqueous solutions such as H_2SO_4 largely independent of aerosol composition [19]. Importantly, the timescale for N_2O_5 removal on tropospheric aerosol is estimated to range from minutes in heavily polluted air, characterised by increased particle density and surface area, to hours in more remote regions [16].

Owing to the human health impact of $PM_{2.5}$, significant reductions in direct $PM_{2.5}$ and gaseous precursor emissions have been appended to many global air pollution policies, and relative concentrations have begun decreasing. Following significant $PM_{2.5}$ decreases in Beijing, China, from 2013, a non-linear relationship of $PM_{2.5}$ and O_3 between the years of 2013 and 2017 was recently reported [20]. Their observations showed that in highly polluted regions (i.e., high $PM_{2.5}$ concentrations), the aerosol chemistry involving reactive uptake of the gaseous precursors (e.g., HO_2) dominated over the loss of HO_2 by NO, resulting in decreased ozone formation. Significant reductions in $PM_{2.5}$ since the State Council of China enacted the Clean Air Action Plan in 2013 were postulated to have induced a rise in surface-level O_3, due to reduced reactive uptake of HO_2. The GEOS-Chem model simulation results were also found to be in agreement with this postulation, attributing most of the observed suppression to HO_2 radical-scavenging by $PM_{2.5}$ [20]. To compliment the observational evidence presented in the study by Li et al. [20], a corresponding study has been performed using measurement data from UK sites.

In 2010, the UK published Air Quality Standards Regulations (AQSR) which prompted national $PM_{2.5}$ reduction measures, including a specific annual average concentration aim to be met by 2020 [21]. In UK urban areas, the yearly average $PM_{2.5}$ concentrations are decreasing over time due to pollution control strategies [22] and ground-level O_3 concentrations were reported to have been increasing over the preceding decade [23–25]. However, the current levels of $PM_{2.5}$ in urban sites still exceed legislation. Using UK Automatic Urban and Rural Monitoring Network (AURN) hourly measured data for a 10-year period beginning from 2010, this study analysed the impact of UK $PM_{2.5}$ emission reductions on ground-level O_3 concentrations, which were reported to be rising in the UK according to the most recent UK Air Quality Expert Group (AQEG) report in 2021 [23]. Therefore, this study aims to assess the impact of $PM_{2.5}$ reductions on the ground-level O_3 increases in the UK, using observational data from the 10-year period following the publication of the 2010 AQSR. Findings from this study will be important in guiding future air pollution policies and reduction strategies involving both O_3 and $PM_{2.5}$ in the UK, which will be beneficial in terms of improved quality of life, for both people and ecosystems.

2. Materials and Methods

2.1. Measurement Data

Measured data of O_3, NO_x, and $PM_{2.5}$ concentrations were extracted for the 10-year period from January 2010 to December 2019 from the UK's national compliance monitoring network, the AURN data archive [26]. The data selection specifically avoided measurements taken during the COVID-19 pandemic and associated lockdowns that may skew pollutant analyses. The AURN is supported by the UK's Department for Environment, Food and Rural Affairs (DEFRA); it records measurement data for a number of air pollutants across 170 air quality monitoring sStations (AQMS) [27].

For O_3 and NO_x concentrations, the measurement techniques used by AURN are UV absorption and chemiluminescence, respectively [26]. For particulate matter measurements, the standard gravimetric reference method does not facilitate continuous on-line monitoring [28]. This is due to the time delay introduced from the requirement to weigh the exposed filters before the analysis of results can take place. In order to supply near-real-time, hourly information on $PM_{2.5}$ concentrations, the AURN instead uses automated measuring systems accepted to be equivalent to the reference method, in accordance with the automated techniques standard. The AURN employs six equivalent techniques: 'Tapered Element Oscillating Microbalance (TEOM)', 'Beta Attenuation monitor (BAM)', 'Gravimetric monitor (GM)', 'Filter Dynamics Measurement System (FDMS)', 'Optical light scattering (OLS)', and 'Fine Dust Analysis System (FIDAS)'. The instruments all have a minimum performance criterion of 25% measurement uncertainty, which also accounts for natural measurement fluctuations. In addition, $PM_{2.5}$ concentration measurements require valid data capture of at least 85%. Data validation consists of a manual review of the data, ensuring use of the most recent calibration factors for data scaling [29]. Additionally, validation excludes any data obtained during instrument malfunctions or faulty calibrations, but incorporates any data missed due to monitoring station communication failures.

The daily mean NO_x and $PM_{2.5}$ data were calculated from measured hourly concentrations. The measured O_3 data were obtained as the daily maximum 8 h running mean (MDA8), which is the maximum 8 h running mean measured on a specific day, from midnight to midnight [30]. The calculation progresses with a one-hour step, generating running mean values for intervals such as 00:00–07:59 or 01:00–08:59. Consequently, a total of 24 values for 8 h running means is possible within a day, but 75% valid data capture is required for a valid running mean. The highest (maximum) mean value is selected from the valid calculated values. MDA8 data are used for O_3 because production occurs during daylight hours and are suppressed during the night-time. DEFRA's Automatic Hydrocarbon Network employs an automated PerkinElmer gas chromatograph to monitor 29 VOCs (12 alkanes, 10 olefins, 1 alkyne, and 6 aromatic hydrocarbons) at an hourly resolution [31]. More details about the VOCs can be found in Table A1, Appendix A. VOC

data were extracted specifically for the London Marylebone Road (LMR) Urban Traffic site. Data were extracted as the daily mean in units of $\mu g/m^3$ and have a measurement uncertainty of 15% [31].

2.2. Monitoring Sites

Of the 170 available UK monitoring sites, only those with 6 years or more of sufficient data coverage for the summer season (>70% for June, July, and August) were used in the subsequent analysis, which constituted 46 sites. The selected sites included 5 of the 6 site types used by UK AIR: Rural Background (RB), Suburban Background (SB), Urban Background (UB), Urban Industrial (UI), and Urban Traffic (UT). The percentage representation of each site type varied in the analysis, as did the number of sites in each country (Figure 1). Of the 46 sites included in the analysis, the largest percentage (36 sites, 78%) belonged to the Urban Background site type, and the smallest percentage (2%), consisting of a singular site, belonged to the Suburban Background site type. The remaining 3 site types each comprised 3 sites, accounting for 6.5% of the dataset, respectively. The Suburban Industrial (SI) site type was not included in the analysis due to insufficient measurement data of the relevant pollutants. Of the analysed sites, there were 2 located in Scotland, Northern Ireland, and Wales each. The remainder, and majority (40 sites, 87%), were located in England. All sites outside of England are in close proximity, <25 miles, to the open coast. Additionally, 14 of the sites in England are considered to be within 25 miles of the coast. Hence, a total of 43% of analysed sites are considered to be close to the coast.

The AQMS located at Marylebone Road exemplifies a typical roadside site in London, positioned 1 metre from the six-lane A501 [32–36]. Functioning as a reliable gauge of pollutant concentrations stemming from mobile sources within the Urban Traffic zone of London, this monitoring site is situated adjacent to Regent's Park in the north, while prominent London city blocks surround it in other directions. The nearby vicinity forms a street canyon and encompasses educational institutions, tourist spots, retail establishments, and residential units. Due to Marylebone Road being a heavily trafficked thoroughfare, holding the highest traffic volume in London, it stands as a distinctive location for accurately representing the emission characteristics of the urban area in London [37]. Birmingham is the second most populous urban area in the UK after London [38]. The air quality monitoring station at BAR is located 6.5 metres from the kerb on a part of Birmingham's heavily trafficked ring road [39]. BTR is located just 5 km away from BAR, next to a dual carriageway and ~700 metres to the north of the M6 motorway.

*2.3. Data Analysis*

The data obtained for O_3, NO, and $PM_{2.5}$ for all 46 AQMS were filtered to include summer months (June, July, and August) only, due to peak O_3 concentrations being of most concern in summer weather conditions [40,41]. The summer month data were subsequently sorted according to site type. Individual site data were categorized and averaged across site type, enabling focused site type trend analysis. As the only 'Suburban Background' site, measured data from London Eltham represents this entire site type in the general analysis. 'Urban Traffic', 'Rural Background', and 'Urban Industrial' site type averages were generated from only 3 sites each.

MDA8 O_3 and average daily mean NO were plotted against average daily mean $PM_{2.5}$ to determine their respective relationships. This analysis was conducted for the entire 10-year period for each site type and specific sites of interest. This allowed direct comparison of UT sites to non-UT sites to provide background information on the relationship between O_3-NO and O_3-$PM_{2.5}$ over the UK for the most recent 10-year period that was unaffected by COVID-19. Further site- and year-specific plots were generated, which provided additional information on yearly variations in these relationships at specific sites. Linear regression analysis on an average imputed data set was conducted for each plot, from which line-of-best-fit equations and R^2 values were generated. The imputed data set used the mean concentration where measured concentration values were missing. Site-specific

annual plots were tested for statistical significance at the standard 5% level of uncertainty (95% confidence level). Years where *p*-values were larger than 0.05 were not included in subsequent analyses.
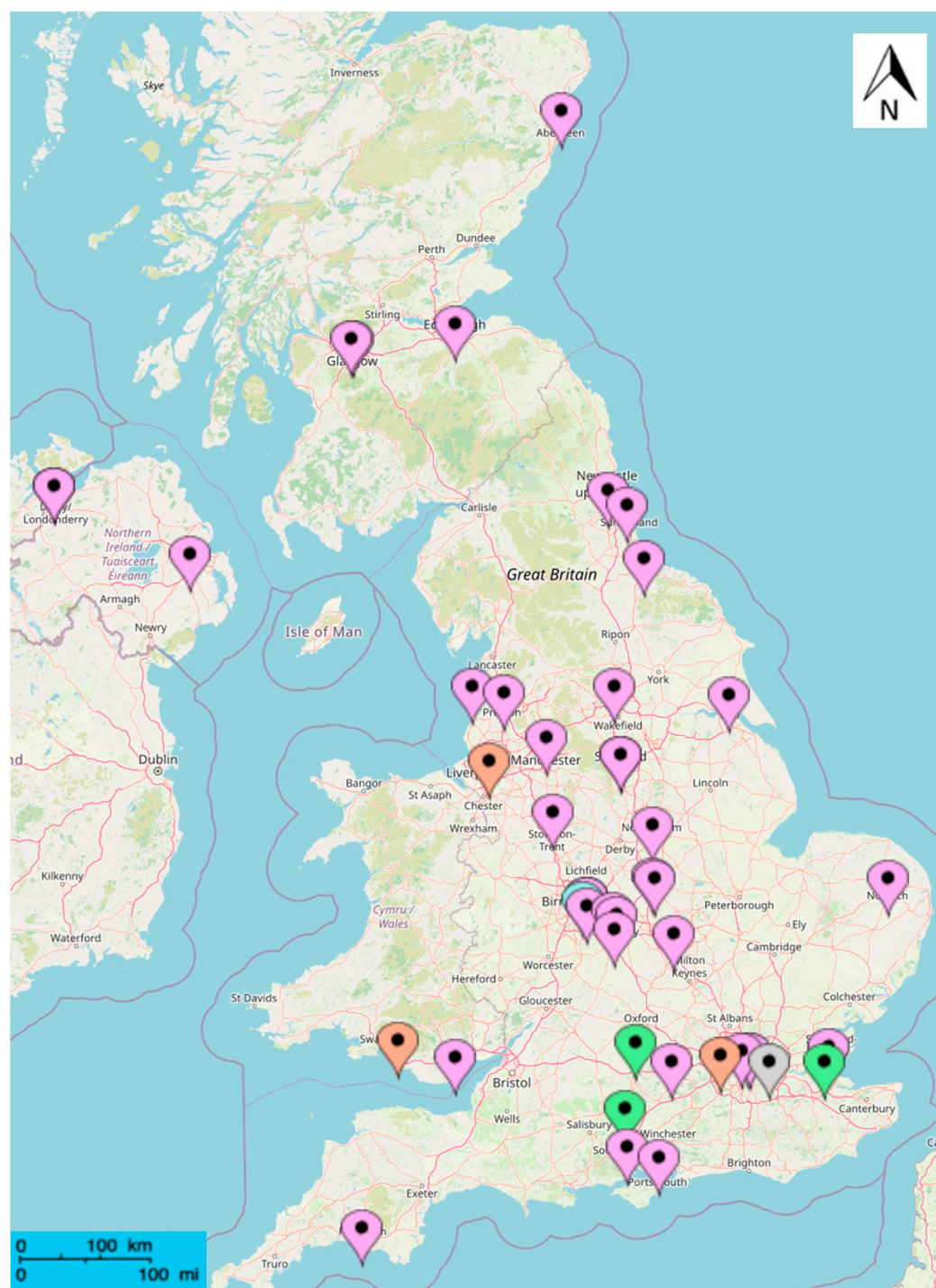
Figure 1. Map of 46 UK sites used in the analysis. Location points are colour coded according to the monitoring station site type (Blue = Urban Traffic, Green = Rural Background, Orange = Urban Industrial, Purple = Urban Background, Grey = Suburban Background) An Urban Traffic site in London is obscured due to overlapping location points. There are 2 Urban Traffic sites overlayed in Birmingham.

Maximum and minimum gradients were calculated using the 95% confidence level values of regression gradient and intercept. This analysis has value as the error analysis for this type of plot, allowing the range of possible gradients and thus pollutant relationships to be depicted. The yearly change in gradient was plotted as a bar chart for the sites where the gradient changed to negative for at least 1 year in the 10-year period.

Timeseries plots of NO_x and $PM_{2.5}$ concentrations, along with summed VOC concentrations where data were available, were plotted for the UT site types over the 10-year period from January 2010 to December 2019. This sequential analysis approach was employed to establish general pollutant concentration trends across the period and to examine year-on-year variations in pollutant levels. Standard error (σ_{x^-}) was calculated from standard deviation (σ) and displayed as error bars on the plots.

3. Results and Discussion

The relationship between NO and $PM_{2.5}$ at the RB, SB, UB, UI, and UT environmental sites is shown in Figure 2. Primary NO_x emissions occur almost exclusively in the form of NO, and due to NO oxidation occurring on a very fast timescale, a positive correlation between NO and $PM_{2.5}$ was taken to indicate a strong primary source of $PM_{2.5}$. As expected, the highly polluted UT environments dominated the axis of Figure 2a. As the most significant UK primary emission source of NO is from car exhausts [42], this site type recorded significantly higher NO concentrations compared with other site types. The largest number of $PM_{2.5}$ measurements above 30 $\mu g\ m^{-3}$ can also be attributed to the UT site type, including the highest $PM_{2.5}$ concentrations recorded. This is indicative of significant primary $PM_{2.5}$ emissions at high traffic sites, a result of both exhaust emissions and non-exhaust emissions, such as tyre and brake wear, road dust, and abrasion [43]. A strong positive correlation indicates NO-$PM_{2.5}$ co-pollution at traffic sites, as well as suggests that primary-emission-focused reduction measures could be successful for reducing both $PM_{2.5}$ and NO in highly polluted environments in the UK.

Excluding the UT site type (Figure 2b) permits a more focused analysis of the other environments. Significant overlap occurred between UB and UI data points, inferring similarly moderate primary sources of $PM_{2.5}$ and NO, likely from domestic emissions and road vehicle emissions at UB sites and from industrial-related emissions at the UI site type. UI and UB sites displayed a general positive NO-$PM_{2.5}$ correlation, indicating relevant primary emission reduction could reduce $PM_{2.5}$ and NO concurrently, analogous to UT sites. In Figure 2b, the higher measured NO concentrations, those exceeding 10 $\mu g\ m^{-3}$, mostly occur at UI and UB site types, but comparatively few high relative $PM_{2.5}$ concentrations are measured, particularly those exceeding 25 $\mu g\ m^{-3}$.

The RB and SB site types show high concentrations of $PM_{2.5}$, despite very low NO concentrations. Sources of NO are much less abundant in rural and suburban regions, predominantly due to a sharp decline in road traffic. In 2017, the UK National Atmospheric Emissions Inventory (NAEI) reported domestic combustion to represent a major source (41.6%) of $PM_{2.5}$ emissions in the UK, but a relatively minute NO_x source (3.9%) [42]. In addition, once formed, $PM_{2.5}$ has a characteristic high susceptibility to movement and thus can easily travel from urban environments to more rural areas before detection, unlike NO. High levels of $PM_{2.5}$ where NO is low could also be indicative of secondary $PM_{2.5}$. High concentrations of biogenic VOCs (BVOC) exist at rural locations and can contribute to significant secondary organic aerosol (SOA) formation. Moreover, these two site types are represented by only four sites in the analysis, of which two (50%) are within a 25-mile radius of the coast, indicating that transported sea spray and dust may comprise a significant contribution to the $PM_{2.5}$ composition.

(**a**)


(**b**)
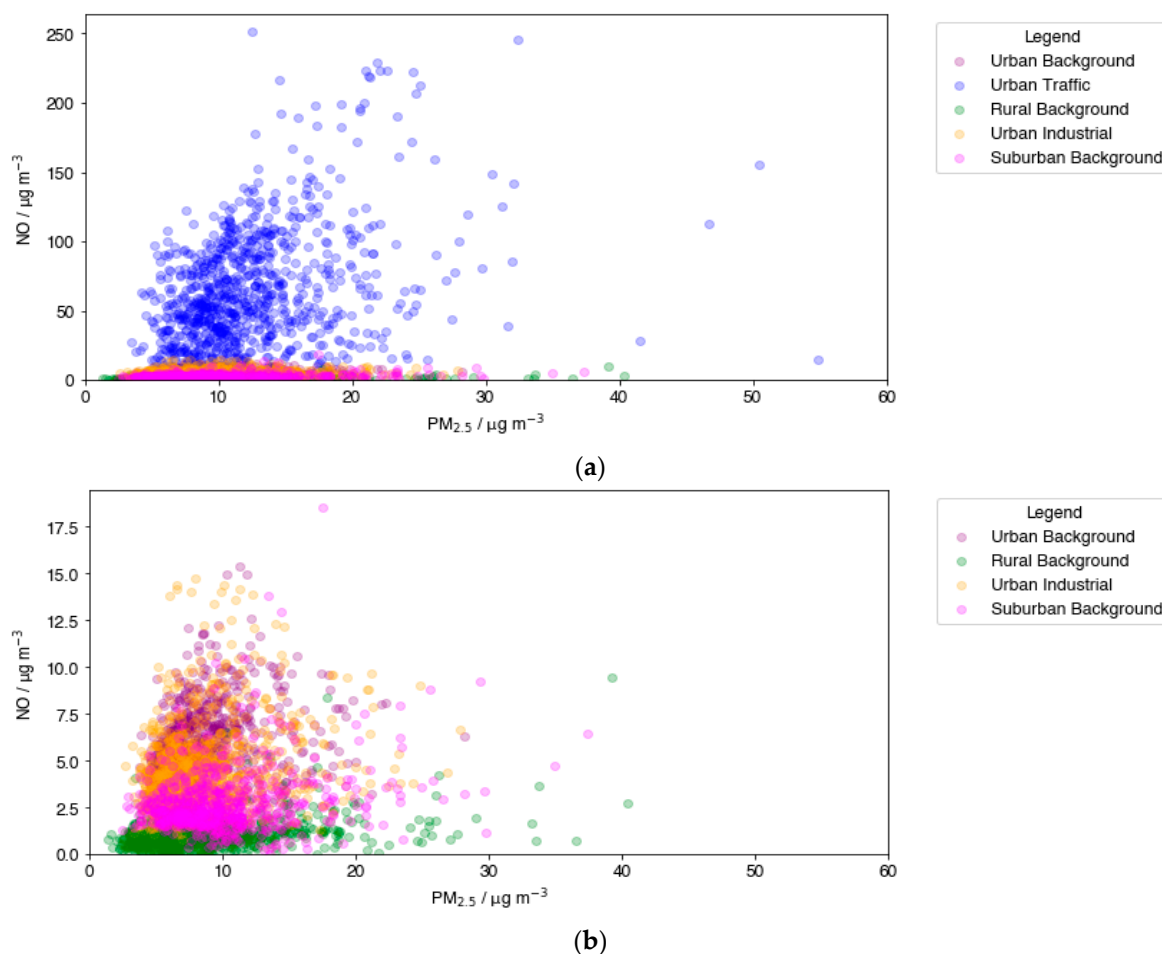
Figure 2. The relationship between NO and PM$_{2.5}$, plotted as daily means across 5 site types in the UK. Plot (**a**) presents data for all site types, Plot (**b**) excludes UT data for better intercomparison for other site types. Data are plotted for summer months (June, July, and August) for a 10-year period between 2010 and 2019. The NO vs. PM$_{2.5}$ plots for individual site types are shown in Appendix B (Figure A1).

The relationship between O$_3$ and PM$_{2.5}$ at each environmental type is displayed in Figure 3. O$_3$ was plotted as MDA8 to account for the strong diurnal variations of the pollutant. O$_3$ is considered to be a secondary pollutant in the boundary layer, formed from photochemical oxidation reactions; thus, co-pollution of O$_3$ and PM$_{2.5}$ is a better indicator of secondary PM$_{2.5}$, which can form as a result of the same OH-initiated reactions as O$_3$.

In Figure 3, the RB site type displays the highest recorded O$_3$ concentrations. High O$_3$ production is characteristic of rural areas in the summer due to the combination of many factors, such as abundant sunlight, elevated temperatures, and elevated biogenic emissions from vegetation. Aligned high PM$_{2.5}$ measurements could be again attributed to SOA formation from the high biogenic VOC emissions in summer and transport from nearby urban areas, which is also likely for the SB sites. High concentrations of both O$_3$ and PM$_{2.5}$ are measured mainly in RB and SB site types. The lowest O$_3$ measurements can be attributed to the UT site type overall, in contrast to what was observed with NO. This suggests that PM$_{2.5}$ sources at UT sites are predominantly primary, as they are more correlated with NO than O$_3$. This agrees with vehicles accounting for a very large urban primary source of both NO and PM$_{2.5}$. By contrast, O$_3$ production efficiency is known to decrease at highly polluted sites, as a result of the extremely elevated NO$_x$ concentrations, which results in O$_3$ formation being VOC-limited [44]. The competitive termination reaction between NO and OH in the ozone-forming photochemical sequence inhibits the initiation

reaction between OH and VOCs. Ozone production efficiency shows linearity to VOC emissions as a result. In the absence of a street canyon structure, higher anthropogenic VOC emissions at urban sites can be effectively balanced by increased atmospheric mixing and dispersion, preventing the ozone precursor's accumulation. In addition, the UK began addressing VOC emissions prior to 2010, with the earliest VOC emission reduction targets being required to be met by 2003 [42]. These factors, with the added fact that urban areas exhibit lower vegetation coverage, resulting in reduced biogenic emissions of VOCs, it is expected that O_3 production would curtail at UT sites. This BVOC factor is even more pronounced in the summer months used in this study, due to the plant response to heat stress and soil moisture deficits, which sees plants increase their BVOC emissions [45].
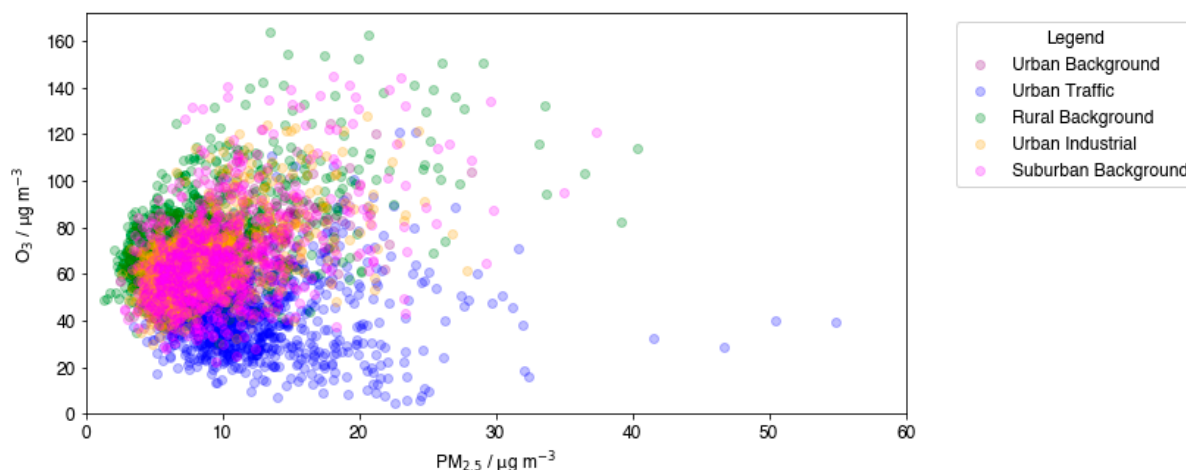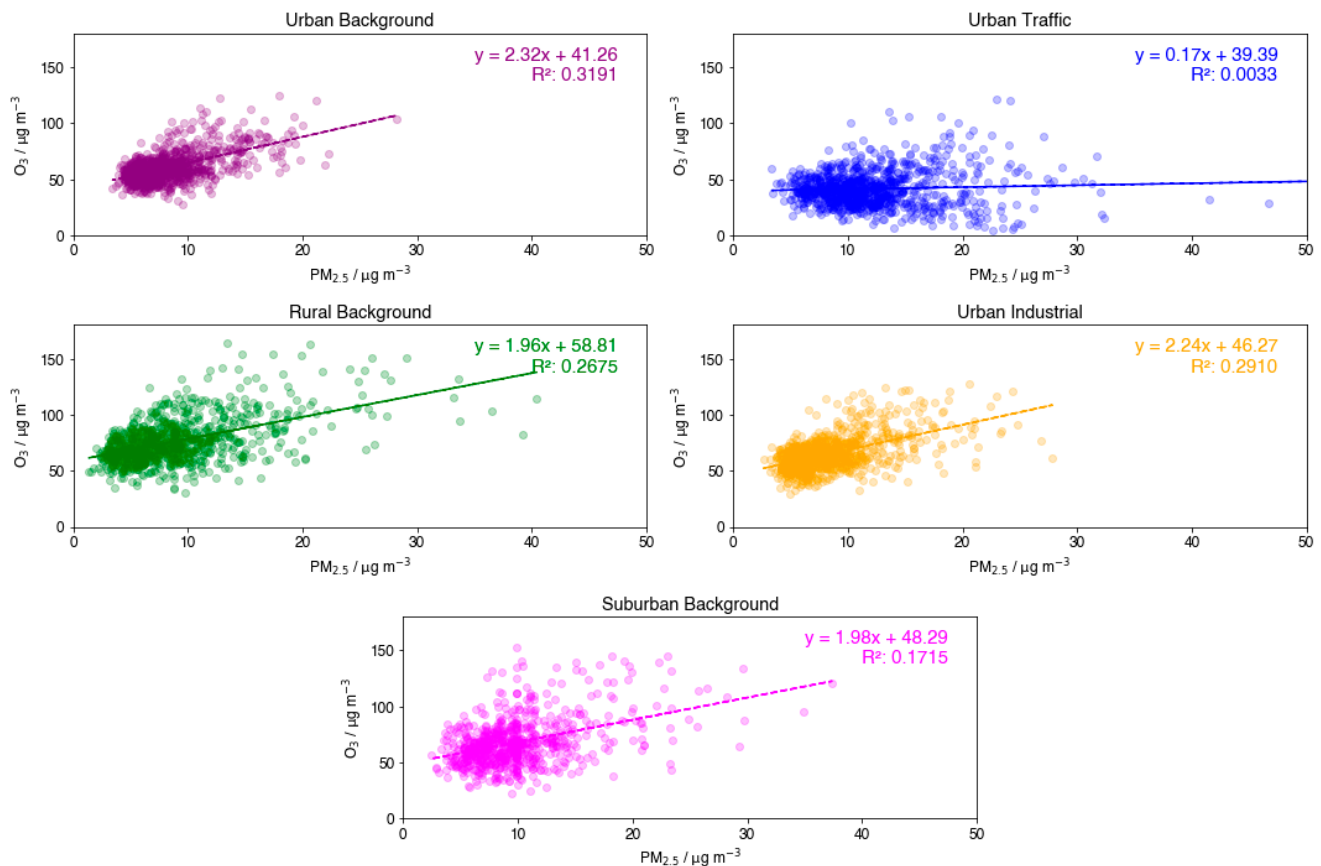

Figure 3. Scatter plots displaying the relationship between daily MDA8 O_3 and $PM_{2.5}$ across 5 site types in the UK.

Despite lower O_3 concentrations at the UT site type, measured $PM_{2.5}$ concentrations still show a much higher average compared with other sites. Linear regression analysis was applied to each site type's individual O_3-$PM_{2.5}$ relationship in Figure 4. Of the five site types, UT is the anomaly in terms of slope and R^2 value, displaying a gradient value around four times lower than other sites and an R^2 value close to zero. There are a significantly larger number of data points at very low O_3 concentrations but moderate to high $PM_{2.5}$ concentrations, ~20 µg m^{-3}. All other site types show a clear positive gradient and thus infer an overall positive relationship between O_3 and $PM_{2.5}$. The spread from the linear regression line at the less anthropogenically polluted site types, SB and RB, is significant, likely reflecting random extreme meteorological events, which have a dependence on specific site location and affect both O_3 formation and transport of primary $PM_{2.5}$ from nearby urban and industrial sources. By contrast, the spread displayed at UB and UI site types is much lower, due to neither site providing optimal conditions for extreme $PM_{2.5}$ or O_3 levels in the summer months. The much shallower gradient is observed for the UT site type.

Three UT sites were included in the analysis: Birmingham A4540 Roadside (BAR), Birmingham Tyburn Roadside (BTR), and London Marylebone Road (LMR). Comparison of O_3 vs. $PM_{2.5}$ scatter plots at the three UT sites (Appendix B, Figure A2) show that both Birmingham sites demonstrate a positive correlation between pollutants. Conversely, the overall correlation at LMR is negative. Given the negative correlation between $PM_{2.5}$ and O_3 seen at LMR, it can be inferred that reducing $PM_{2.5}$ concentrations may play a part in increased O_3 ground-level concentrations in summer months as has been observed in Beijing, China [20]. Further dissection of this relationship on an annual basis demonstrated a clear 'tipping point' at which LMR moves from a statistically significant negative correlation (2014–2015) to a statistically significant positive correlation in recent years (2019) (Figure 5).

Figure 4. Individual subplots displaying the relationship between daily MDA8 O_3 and $PM_{2.5}$ for each site type, including linear regression lines with their equations and R^2 values.
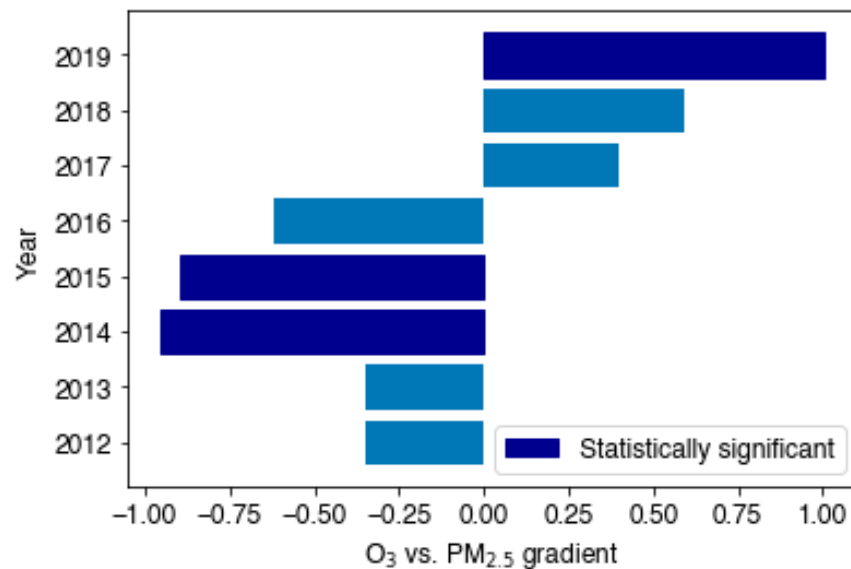

Figure 5. A horizontal bar graph depicting the changing O_3 vs. $PM_{2.5}$ gradients across the 10-year period at LMR, where data coverage was sufficient (>70%). Statistically significant annual plots at the 95% confidence level are shown in navy blue.

Negative correlations, of varying extent, between MDA8 O_3 and mean daily $PM_{2.5}$ were observed over the summer season for the years 2012–2016 at LMR. On average, on days where $PM_{2.5}$ concentrations were highest, MDA8 O_3 concentrations were suppressed,

and vice versa. At the confidence level of 95%, 2014, 2015, and 2019 linear regressions were statistically significant. Additionally, the negative linear regression in 2013 showed statistical significance at the 90% confidence level. The horizontal bar chart in Figure 5 depicts the annual change in the average O_3-$PM_{2.5}$ relationship; an inversion from 2016 to 2017 is clearly shown. The largest negative gradients occurred in the summers of 2014 and 2015; the largest positive gradient occurred most recently in 2019.

To infer the significance of $PM_{2.5}$ reductions on the observed annual O_3 vs. $PM_{2.5}$ relationships and the 2017 inversion, a timeseries plot of mean annual $PM_{2.5}$ concentrations was plotted (Figure 6), including the data from all seasons. Overall, the timeseries plot shows a decrease across the time period. $PM_{2.5}$ peaked at 24.4 µg m^{-3} in 2011 and dropped by 40.6% to 14.5 µg m^{-3} in 2019. The sharpest decrease occurred from 2011 to 2015, where a 35% decline was observed, accounting for 86% of the total decrease. From 2015 to 2018, mean $PM_{2.5}$ stabilised at approximately 16 µg m^{-3}. A further absolute decrease of 1.34 µg m^{-3} was observed from 2018 to 2019.
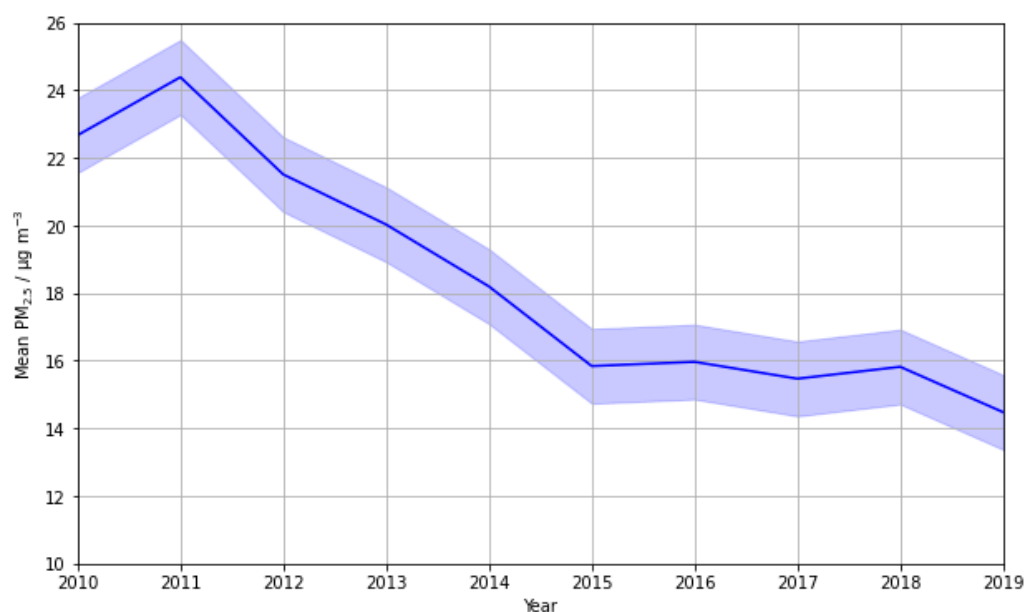
Figure 6. A timeseries plot showing the 10-year trend in average mean daily $PM_{2.5}$ from 2010 to 2019 at LMR. Uncertainty is presented as standard error and represented using a continuous, translucent error bar.

Scatter plots depicting the summer correlations between $PM_{2.5}$ and O_3 specifically for the years 2014, 2015, and 2019 at LMR are shown in Figure 7. The summer period is of particular interest because MDA8 O_3 is enhanced in summer months because of increased temperatures and sunlight intensity, whereas secondary $PM_{2.5}$ tends to be lower. To this notion, it is important to recognise that large MDA8 O_3 measurements can occur as a result of such meteorological conditions, characteristic of the hotter summer days. The year 2015 directly proceeds the most significant decrease (35%) in mean $PM_{2.5}$, which could explain the strong negative gradient seen in Figure 7b. The preceding year, 2014, also shows a strong negative gradient (Figure 7a), following a reduction of 25% from 2011. The 8.5% decrease observed between 2018 and 2019 is not sufficient to cause a relationship inversion (Figure 7c). This suggests that the negative relationship between $PM_{2.5}$ and O_3 is most significant immediately following the steepest decreases in $PM_{2.5}$. The 2018 to 2019 decrease is preceded by a 4-year period of relative stability, further supporting this theory.
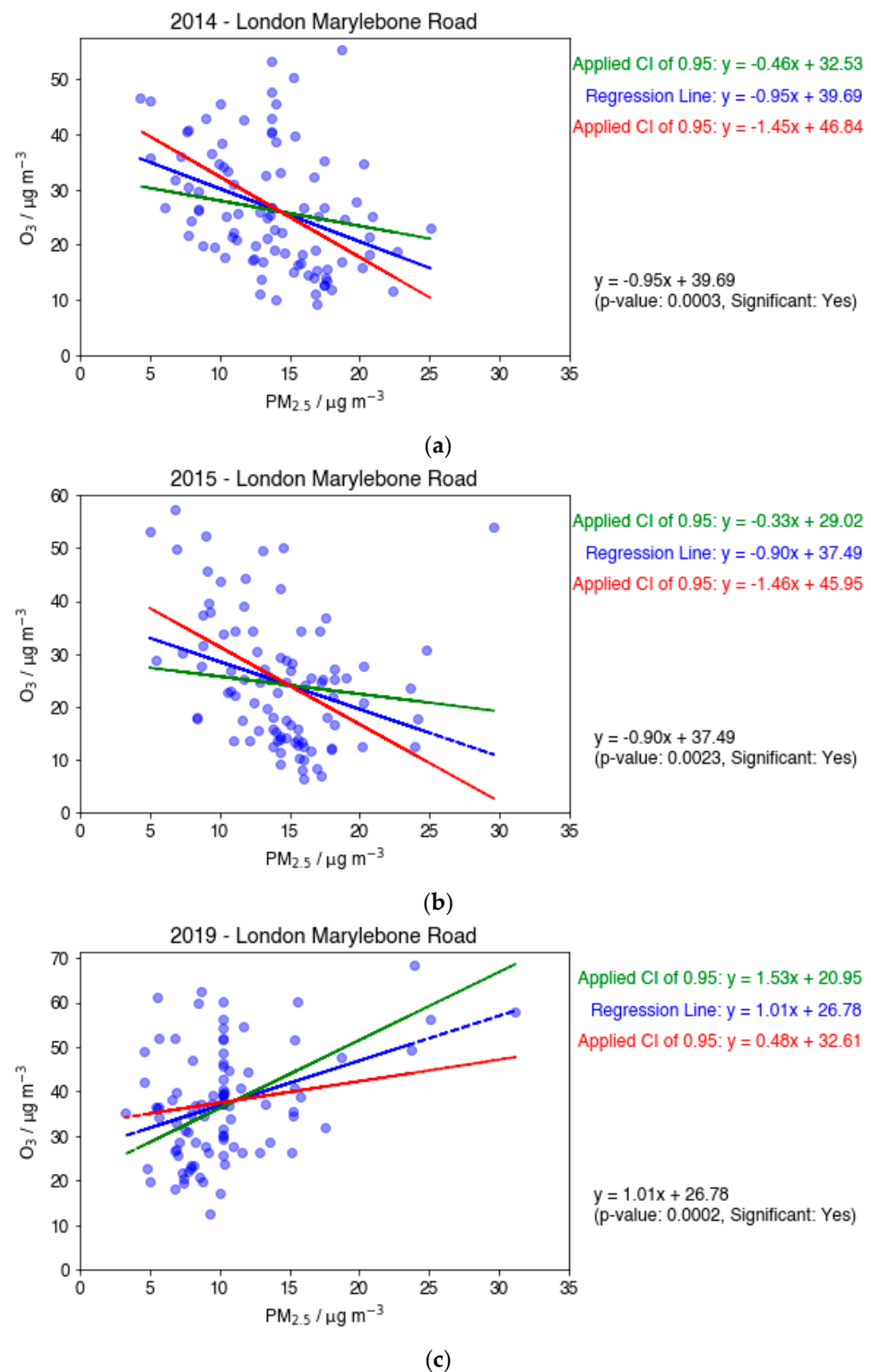
Figure 7. Scatter plots showing MDA8 O_3 against $PM_{2.5}$ for the years 2014 (**a**), 2015 (**b**), and 2019 (**c**) at LMR. The plots include a linear regression line, as well as maximum and minimum linear regression lines at the 95% confidence level. An anomalous $PM_{2.5}$ data point is circled in orange in (**b**).

Error analyses conducted on these plots take the form of maximum and minimum regression lines. In each case, the maximum and minimum gradients align with the original regression gradient sign, which increases confidence in the observed correlation.

Plots 7a,b show similar spreads, both of which suggest that significant reductions in $PM_{2.5}$ are contributing to O_3 spikes.

Figure 7b shows an anomalous value at both high $PM_{2.5}$ and high O_3, which occurred on 12 June 2015. The highest measured O_3 concentrations in the summer of 2015 were all recorded within a 2-week timeframe of 2–15 June; thus, it is likely that these measurements resulted from favourable weather conditions for O_3 formation across this 2-week period, and it is unlikely that the 12 June O_3 measurement was anomalous. However, the result appears to be anomalous in $PM_{2.5}$. The mean and standard deviation values were calculated with both the 12 June measurement included and omitted, respectively, specifically for the days in the 2-week period of early June where O_3 concentrations of 50 µg m^{-3} and higher were recorded. The $PM_{2.5}$ value recorded on 12 June was in excess of two standard deviations from the mean when included in both calculations and larger than five standard deviations from the mean when omitted from the calculations. As a result, this point (circled in orange on Figure 7b) was considered anomalous in $PM_{2.5}$ and disregarded. Removing this data point reveals an even stronger negative correlation in 2015.

At sites classified as UT, the surplus to background $PM_{2.5}$ concentrations can largely be attributed to vehicular emissions [46]. Emission reduction measures that focus on vehicular $PM_{2.5}$ emissions would reduce both primary $PM_{2.5}$ emissions whilst also simultaneously causing reductions in vehicular NO_x emissions. NO_x plays an important role as a gaseous precursor to secondary inorganic and organic nitrate formation in addition to O_3 formation. In a VOC-limited regime, typical of highly polluted urban centres, significant NO_x reductions cause O_3 to spike [22,23]. It is therefore possible that the increase in O_3 could be an effect of NO_x-VOC-O_3 chemistry, caused by the reductions in NO_x that occur simultaneously to reductions in $PM_{2.5}$, rather than as a result of the $PM_{2.5}$ reductions.

The 10-year trend in mean NO_x at the LMR site was plotted and is shown in Figure 8a. An overall decrease across the entire 10-year period is observed. Average NO fluctuations largely mirrored those of overall NO_x, whilst average measured NO_2 showed a dampened, smoother overall decrease. The NO_x trend shows negligible overall change between the years 2010 and 2017, before decreasing significantly in the last 2 years studied. Sectioning the NO trend in the same way reveals a small average increase between 2010 and 2017, before an analogous sharp decrease to 2019. The lack of a substantial decrease in NO_x indicates that O_3 increases were unlikely the result of decreasing NO_x. Additionally, this suggests that the $PM_{2.5}$ decreases were not predominantly a result of NO_x precursor emission reductions reducing secondary organic and inorganic particulate nitrate. This is in agreement with a modelling study conducted by Vieno et al. [47] which showed primary $PM_{2.5}$ reductions to be the most impactful on overall $PM_{2.5}$ reductions in the UK. The initial period of average NO increase is the same period where negative relationships are seen between O_3 and $PM_{2.5}$ at LMR, further supporting this. The observed dip in NO_x occurring from 2012 to 2013, amounting to a 10.6% decline, may have positively influenced the strength of the negative relationship between $PM_{2.5}$ and O_3 though. The same could be said for the 9.2% decrease between 2014 and 2015. However, NO_x peaks in 2014, when the gradient of O_3-$PM_{2.5}$ was the most strongly negative (Figure 7a), suggesting that there is very likely an additional reason why ozone spiked when $PM_{2.5}$ was reduced, not linked to NO_x. This is in agreement with the results reported in China [20,48].

LMR is one of the few sites where measurements of VOCs are taken by the Automatic Hydrocarbon Network. Figure 8b compares the yearly mean measured NO and NO_2 to that of the summed concentration of measured VOCs. Simultaneous reduction in VOCs and NO_x is a widely used pollution reduction strategy in VOC-limited environments where considerable NO_x reductions on their own are known to cause O_3 spikes [49,50]. An overall steady decrease in average summed VOC concentrations of 25% was observed across the 10-year period at LMR. The steeper observed NO and NO_2 decreases between 2012–2013 and 2014–2015 were both accompanied by comparative steep gradient decreases in VOCs, 13.6% and 20.2%, respectively. This is in line with the UK Government introducing strategies to reduce road-traffic-related emissions in 2010, as these emissions comprise

the UK's largest share of both VOC emissions and NO_x emissions [51,52]. This analysis, together with the assumption that LMR exists in a typically VOC-limited time period across the time period considered, which additionally considers the ozone formation potential of each VOC, both provide further evidence that the negative correlation observed between $PM_{2.5}$ and O_3 between 2012 and 2016 at LMR was not just a result of NO_X and VOC reductions. From this, the significance of $PM_{2.5}$ reductions becomes increasingly evident.

(a)

(b)
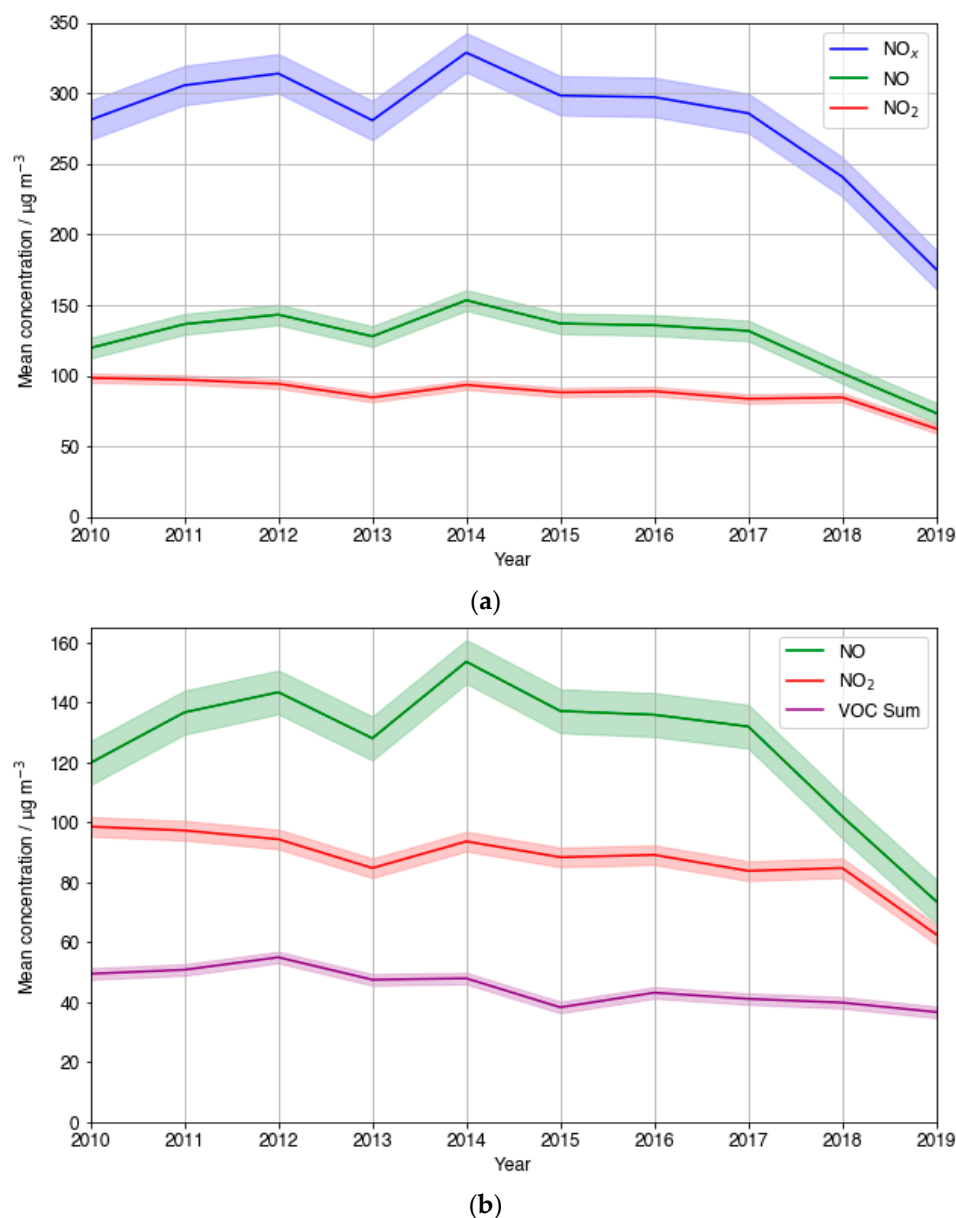
Figure 8. A timeseries plot of the 10-year trend in (**a**) mean NO_X, NO, and NO_2 and (**b**) NO, NO_2, and summed VOC concentrations at LMR.

In contrast to LMR, the other UT sites (BTR and BAR) do not show a negative correlation between $PM_{2.5}$ and O_3 for any individual year within the time period considered. Given the similarities between the three sites, it is important to consider why this result is seen. As BTR was closed down in September 2016, the BAR measurement site just 5 km away was opened as a replacement. Data from the two Birmingham UT sites are therefore combined to provide continuous data for the overall time period. In comparison to LMR, absolute measured $PM_{2.5}$ concentrations were much smaller at BTR and BAR (Figure 9). This is consistent with the results presented by Laxen et al. [53] for 2009 data, where mean

$PM_{2.5}$ concentrations at different site types were compared to the Urban Background mean: mean $PM_{2.5}$ concentrations at kerbside sites (within 1 m of the kerb) of busy roads, such as LMR, averaged values 7–8 µg m^{-3} above Urban Background values, whilst concentrations measured further from the kerb alongside busy roads, such as the Birmingham sites, averaged values only 1–2 µg m^{-3} above the Urban Background mean. With the highest mean $PM_{2.5}$ concentration measured at LMR around 1.5 times larger than that at BTR in this analysis, Birmingham's level of pollution may not exceed the threshold whereby O_3 suppression by $PM_{2.5}$ becomes significant. This is a sensible inference because it is widely accepted that China has one of the most severe air pollution problems, and according to both the studies of Li et al. [20] and Shao et al. [48], many cities in urban megacity regions displayed the inverse relationship observed in London.
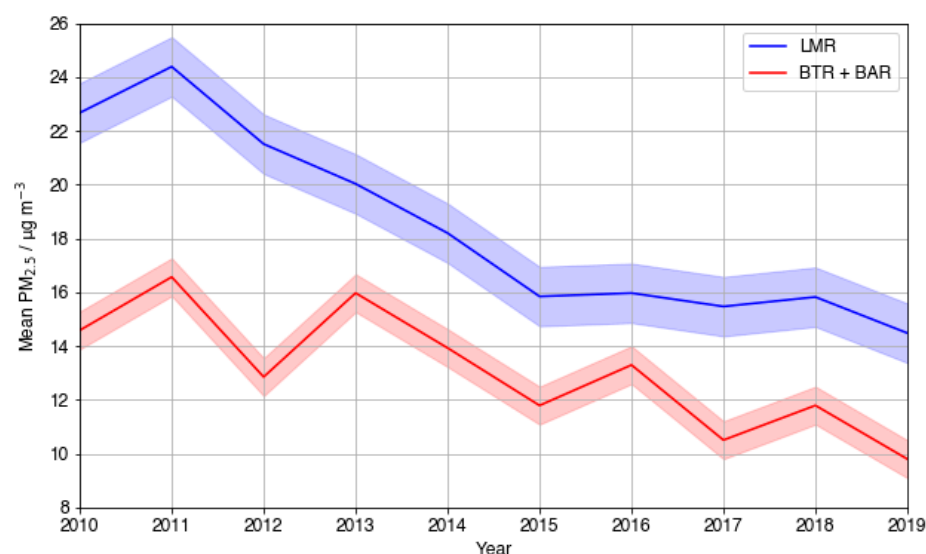

Figure 9. A timeseries plot showing the 10-year trend in average mean daily $PM_{2.5}$ (µg m^{-3}) from 2010 to 2019 at all UT sites: LMR (blue), with BAR and BTR combined (red).

The lower $PM_{2.5}$ concentrations at the Birmingham sites may result from the specific context of these measurement sites compared with LMR. LMR is known to be influenced by the 'street canyon' effect, where pollution dispersion is reduced, and therefore, the pollutant residence time around the measurement site is increased, so higher concentrations may be recorded [54]. Conversely, the Birmingham sites are not influenced by the street canyon effect, indicating that $PM_{2.5}$ is dispersed more quickly following emission. The build-up of $PM_{2.5}$ to levels sufficient to cause O_3 suppression is therefore less likely at the Birmingham sites. Moreover, both Birmingham measurement site locations are further from the kerb than at LMR, facilitating $PM_{2.5}$ dispersion before detection. This is further evidenced by the fact that average yearly NO_2 concentrations are larger than those of NO at the Birmingham sites (Figure 10), which infers conversion of NO to NO_2 before detection. An analysis of additional measurement sites in different cities across the UK, including those affected and unaffected by the street canyon effect, would allow the impact of street canyons on the $PM_{2.5}$-O_3 relationship to be studied further, though only the sites presented here are currently available for a long-term analysis.

VOC concentration measurements are not available for either of the Birmingham UT sites; therefore, investigation into the O_3 formation sensitivity regime is not possible. However, it is likely that the polluted urban centre of Birmingham resides in a VOC-limited regime, consistent with an analysis of other urban centres in the UK, like Edinburgh [55]. From this, it is possible to infer that $PM_{2.5}$ must be present in greater concentrations than the maximum concentrations measured at the Birmingham sites (on average, 17 µg m^{-3}) in order to suppress O_3 formation. Similarly, the same long-term (>2 years), steep decreases in

PM$_{2.5}$ concentrations seen at LMR were not present at the Birmingham sites; it is possible this is also a requirement to see PM$_{2.5}$-mediated O$_3$ spikes in urban centres in the UK.
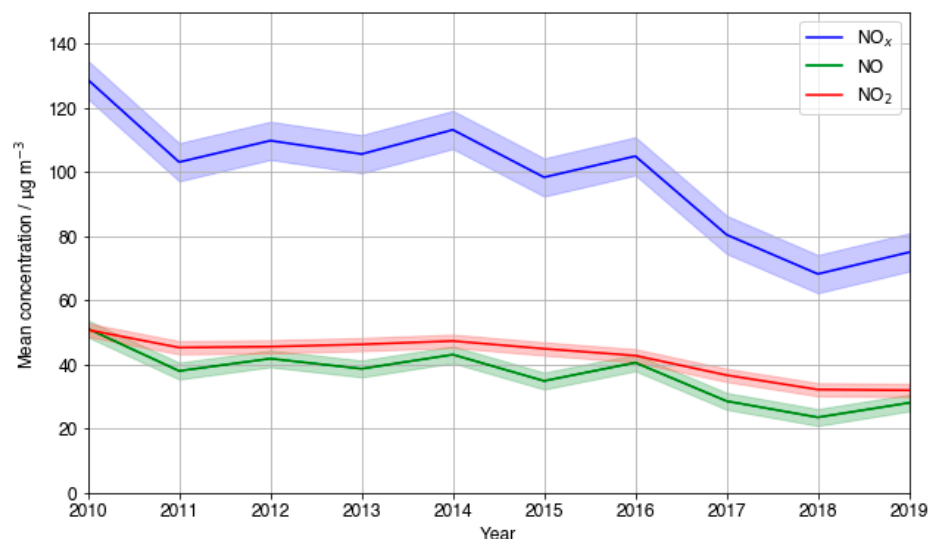
Figure 10. The 10-year trend in mean, combined NO$_x$, NO, and NO$_2$ in µg m^{-3} at the Birmingham sites.

These results have implications for air pollution policy in the UK and across the globe. Quantifying the threshold PM$_{2.5}$ concentration above which O$_3$ suppression is significant for different UT environments, such as those impacted by street canyon effects, would hugely benefit the policies that target specific air pollution hotspots. Air pollution reduction strategies in VOC-limited urban centres where PM$_{2.5}$ concentrations additionally exceed the PM$_{2.5}$ threshold could utilise combined, gradual-decrease control strategies with all three pollutants in order to effectively mitigate O$_3$ spikes [20]. In areas where the PM$_{2.5}$ threshold is not exceeded, current strategies that aim for maximum reduction in PM$_{2.5}$, without favouring one of either NO$_x$ or VOC reductions, would be most efficient and could significantly reduce PM$_{2.5}$ population exposure. With recent studies showing that there exists no PM$_{2.5}$ concentration below which negative health effects cease, this strategy could significantly improve the health of the nation [56].

4. Conclusions

This study analysed the relationship between PM$_{2.5}$ and ground-level O$_3$ across the UK to determine if the PM$_{2.5}$ reductions, required by the 2010 AQSR, contributed to increasing surface-level O$_3$ concentrations between the years 2010 and 2019. The largest primary contribution to the PM$_{2.5}$ concentration was observed at the UT site type which had the strongest positive NO-PM$_{2.5}$ relationship, confirming the impact of road vehicle traffic emissions on local pollution. Additionally, the O$_3$-PM$_{2.5}$ relationship at the UT site type showed a much weaker correlation in comparison to the other site types, confirming the importance of primary PM$_{2.5}$ at this site type. A much larger secondary contribution to PM$_{2.5}$ was observed at the other site types, which is more closely correlated to O$_3$ formation due to similar favourable conditions for gaseous precursor photochemistry. Establishing the 10-year decreasing trend in PM$_{2.5}$ at LMR indicated that surface-level O$_3$ concentrations were increasing as PM$_{2.5}$ concentrations were decreasing. LMR is considered to be in a VOC-limited regime; thus, it is possible that simultaneous NO$_X$ reductions were responsible for O$_3$ spiking, rather than PM$_{2.5}$ reductions. However, overall, NO$_X$ fluctuations were found to be minimal and were accompanied by VOC decreases; they were shown to have little impact during the years where a negative O$_3$-PM$_{2.5}$ relationship was observed. In contrast to LMR, neither Birmingham site displayed a negative O$_3$-PM$_{2.5}$ gradient during any of the years analysed. Consideration was given to the lower NO concentrations at the Birmingham sites being indicative of a NO$_X$-sensitive regime, nullifying the effect of PM$_{2.5}$ reductions on O$_3$ when simultaneous NO$_X$ reductions were occurring. This analysis therefore suggests that O$_3$ suppression by PM$_{2.5}$

chemistry is sufficient to cause O_3 increases in the UK when average $PM_{2.5}$ concentrations start above a threshold value, t, where $17 \ \mu g \ m^{-3} < t < 26 \ \mu g \ m^{-3}$ and decrease (by > 26%) continuously over a period of longer than 2 years. In this 2010 to 2019 UK study, LMR was the only analysed site to demonstrate the negative impact of significant $PM_{2.5}$ reductions on surface-level O_3. Exemplifying the street canyon effect, and as the UK's single busiest road in terms of vehicle traffic, LMR measured the highest $PM_{2.5}$ concentrations in this study, likely to be mainly composed of primary $PM_{2.5}$. Other UK city centres where high-rise buildings and traffic are abundant may additionally see this negative O_3-$PM_{2.5}$ relationship. The results obtained in this study therefore indicate the benefit of employing different air pollution reduction strategies in highly trafficked urban centres to those employed across the rest of the UK. In particular, the results evidence the importance of simultaneous VOC reductions for effective joint O_3 and $PM_{2.5}$ reduction strategies in areas of significant primary $PM_{2.5}$. Outside of highly polluted city centres, where the negative O_3-$PM_{2.5}$ relationship appeared not to be a concern, more extreme $PM_{2.5}$ reduction policies can be employed to maximally reduce population exposure to $PM_{2.5}$ and thus significantly reduce its impact on human health. This approach can be extended to other cities across the globe, informing future policy. As secondary pollutants with substantial atmospheric residence times, the largest improvements to the environment and human health will be seen only when effective joint O_3-$PM_{2.5}$ air pollution mitigation strategies are employed in all inhabited regions.

Appendix A

Table A1. Volatile organic compounds (VOC) data extracted from DEFRA's Automatic Hydrocarbon Network used in the analysis.

Alkanes	Alkenes	Alkyne	Aromatic
Ethane	Ethene	Ethyne	benzene
Propane	Propene		toluene
iso-butane	1-butene		ethylbenzene
n-butane	trans-2-butene		m+p-xylene
iso-pentane	cis-2-butene		o-xylene
n-pentane	1,3-butadiene		1,2,3-trimethylbenzene
2-methylpentane	trans-2-pentene		
n-hexane	1-pentene		
n-heptane	isoprene		
iso-octane	cis-2-pentene		
n-octane			
3-methylpentane			

Appendix B
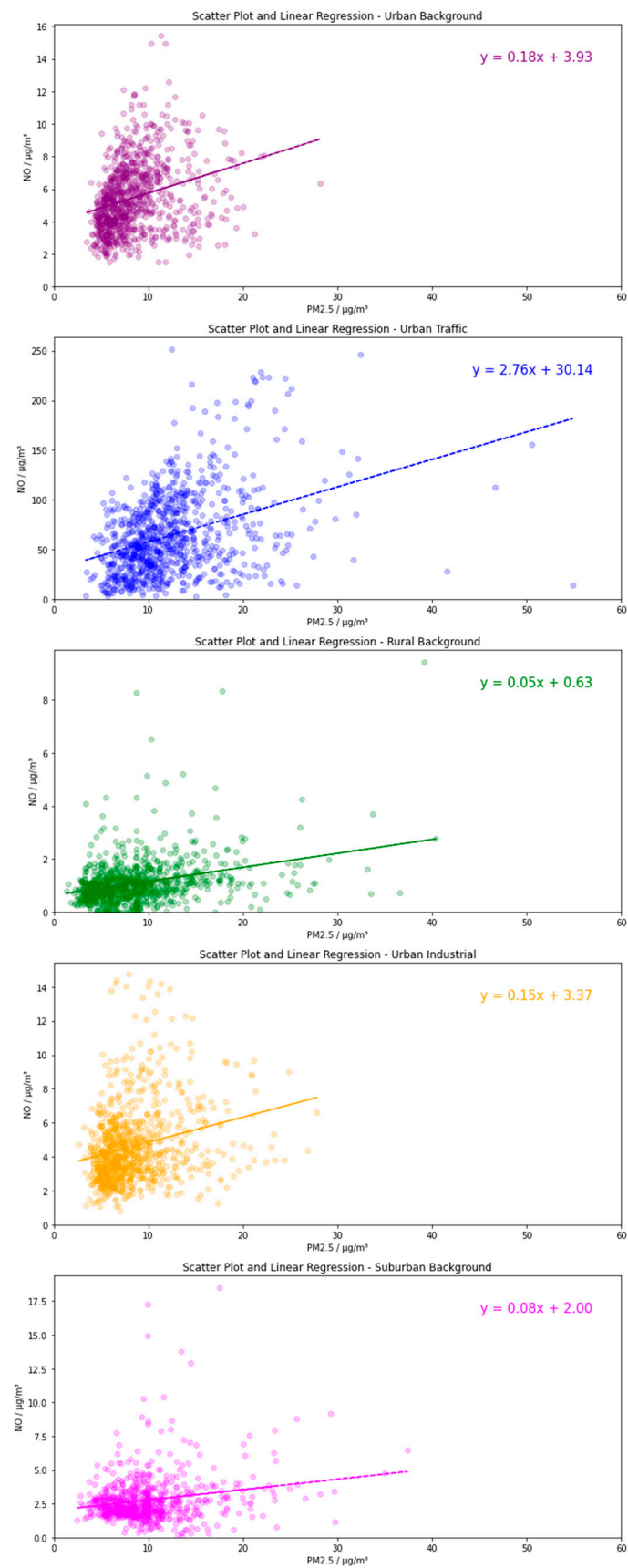
Figure A1. The relationship between NO and PM$_{2.5}$ for individual site types.
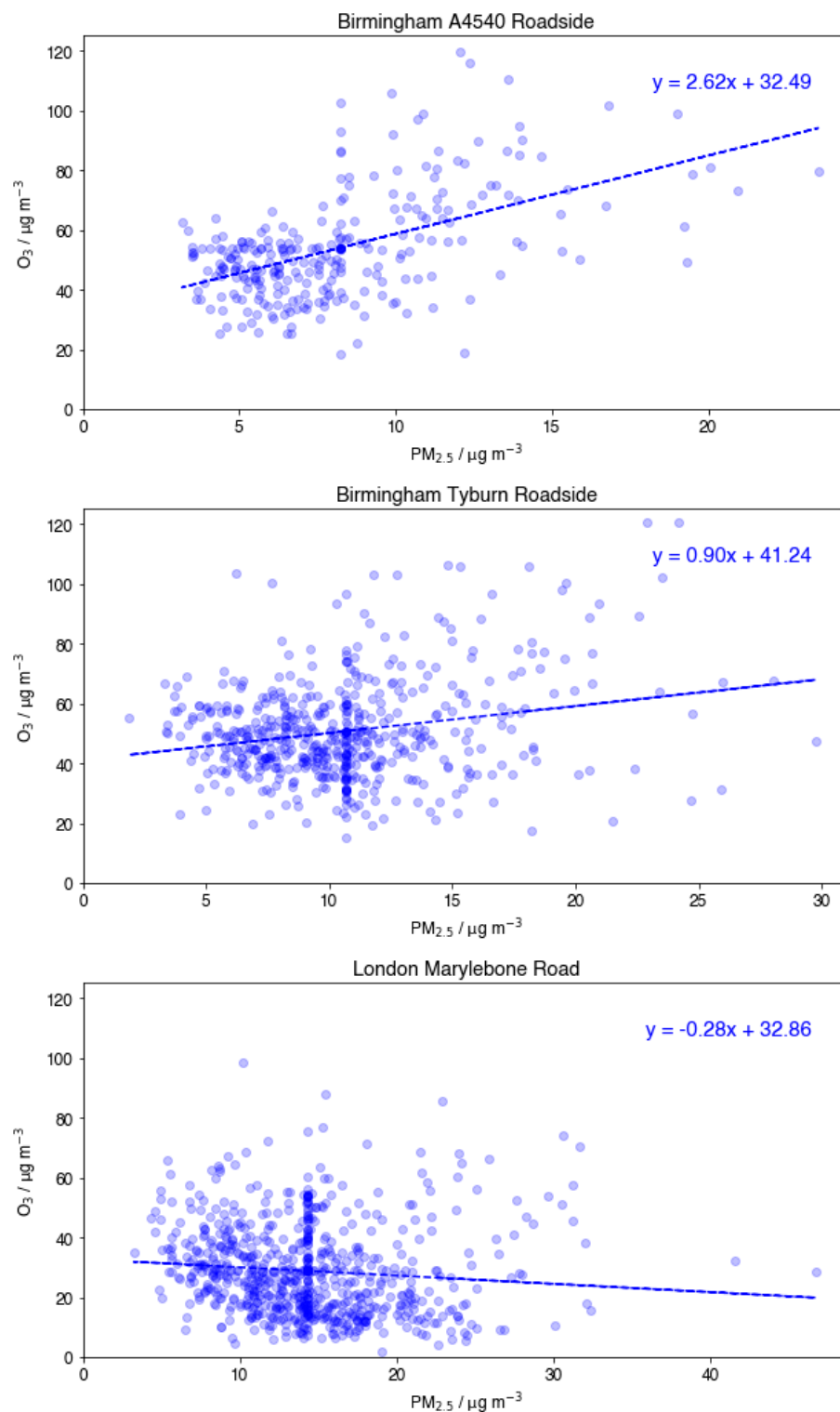
Figure A2. Comparison of O$_3$ vs. PM$_{2.5}$ scatter plots at Birmingham A4540 Roadside, Birmingham Tyburn Roadside, London Marylebone Road.

References

1. Oh, M.-S.; Park, C.K. Regional source apportionment of PM$_{2.5}$ in Seoul using Bayesian multivariate receptor model. *J. Appl. Stat.* **2022**, *49*, 738–751. [CrossRef] [PubMed]
2. Samek, L.; Stegowski, Z.; Furman, L.; Styszko, K.; Szramowiat, K.; Fiedor, J. Quantitative assessment of PM$_{2.5}$ sources and their seasonal variation in Krakow. *Water Air Soil Pollut.* **2017**, *228*, 290. [CrossRef] [PubMed]

3.   Chow, W.S.; Liao, K.; Huang, X.H.H.; Leung, K.F.; Lau, A.K.H.; Yu, J.Z. Measurement report: The 10-year trend of $PM_{2.5}$ major components and source tracers from 2008 to 2017 in an urban site of Hong Kong, China. *Atmos. Chem. Phys.* **2022**, *22*, 11557–11577. [CrossRef]

4.   Philip, S.; Martin, R.V.; Snider, G.; Weagle, C.L.; van Donkelaar, A.; Brauer, M.; Henze, D.K.; Klimont, Z.; Venkataraman, C.; Guttikunda, S.K.; et al. Anthropogenic fugitive, combustion and industrial dust is a significant, underrepresented fine particulate matter source in global atmospheric models. *Environ. Res. Lett.* **2017**, *12*, 044018. [CrossRef]

5.   Ditto, J.C.; Joo, T.; Khare, P.; Sheu, R.; Takeuchi, M.; Chen, Y.; Xu, W.; Bui, A.A.T.; Sun, Y.; Ng, N.L.S.; et al. Effects of Molecular-Level Compositional Variability in Organic Aerosol on Phase State and Thermodynamic Mixing Behavior. *Environ. Sci. Technol.* **2019**, *53*, 13009. [CrossRef] [PubMed]

6.   McDuffie, E.E.; Martin, R.V.; Spadaro, J.V.; Burnett, R.; Smith, S.J.; O'Rourke, P.; Hammer, M.S.; van Donkelaar, A.; Bindle, L.; Shah, V.; et al. Source sector and fuel contributions to ambient $PM_{2.5}$ and attributable mortality across multiple spatial scales. *Nat. Commun.* **2021**, *12*, 3594. [CrossRef] [PubMed]

7.   Department for Environment Food and Rural Affairs. Air Quality Expert Group, Fina Particulate Matter (PM2.5) in the United Kingdom. Available online: https://uk-air.defra.gov.uk/research/aqeg/ (accessed on 14 May 2024).

8.   Beekmann, M.; Prévôt, A.S.H.; Drewnick, F.; Sciare, J.; Pandis, S.N.; Denier van der Gon, H.A.C.; Crippa, M.; Freutel, F.; Poulain, L.; Ghersi, V.; et al. In situ, satellite measurement and model evidence on the dominant regional contribution to fine particulate matter levels in the Paris megacity. *Atmos. Chem. Phys.* **2015**, *15*, 9577–9591. [CrossRef]

9.   De Meij, A.; Thunis, P.; Bessagnet, B.; Cuvelier, C. The sensitivity of the CHIMERE model to emissions reduction scenarios on air quality in Northern Italy. *Atmos. Environ.* **2009**, *43*, 1897–1907. [CrossRef]

10.   Larsen, B.; Gilardoni, S.; Stenström, K.; Niedzialek, J.; Jimenez, J.; Belis, C. Sources for PM air pollution in the Po Plain, Italy: II. Probabilistic uncertainty characterization and sensitivity analysis of secondary and primary sources. *Atmos. Environ.* **2012**, *50*, 203–213. [CrossRef]

11.   Hodan, W.M.; Barnard, W.R. *Evaluating the Contribution of $PM_{2.5}$ Precursor Gases and Re-Entrained Road Emissions to Mobile Source $PM_{2.5}$ Particulate Matter Emissions*; MACTEC Federal Programs: Research Triangle Park, NC, USA, 2004.

12.   Zhang, J.; Wei, Y.; Fang, Z. Ozone pollution: A major health hazard worldwide. *Front. Immunol.* **2019**, *10*, 2518. [CrossRef]

13.   Nuvolone, D.; Petri, D.; Voller, F. The effects of ozone on human health. *Environ. Sci. Poll. Res.* **2018**, *25*, 8074–8088. [CrossRef] [PubMed]

14.   IPCC. *Climate Change 2013: The Physical Science Basis. Contribution of Working Group I to the Fifth Assessment Report of the Intergovernmental Panel on Climate Change*; Stocker, T.F., Qin, D., Plainer, G.-K., Tignor, M., Allen, S.K., Boschung, J., Nauels, A., Xia, Y., Bex, V., Midgley, P.M., Eds.; Cambridge University Press: Cambridge, UK; New York, NY, USA, 2013.

15.   Juráň, S.; Grace, J.; Urban, O. Temporal changes in ozone concentrations and their impact on vegetation. *Atmosphere* **2021**, *12*, 82. [CrossRef]

16.   Jenkin, M.E.; Clemitshaw, K.C. Ozone and other secondary photochemical pollutants: Chemical processes governing their formation in the planetary boundary layer. *Atmos. Environ.* **2000**, *34*, 2499–2527. [CrossRef]

17.   Colvile, R.N.; Choularton, T.W.; Gallagher, M.W.; Wicks, A.J.; Downer, R.M.; Tyler, B.J.; Storeton-West, K.J.; Fowler, D.; Cape, J.N.; Dollard, G.J.; et al. Observation on great dun fell of the pathways by which oxides of nitrogen are converted to nitrate. *Atmos. Environ.* **1994**, *28*, 397–408. [CrossRef]

18.   Van Doren, J.M.; Watson, L.R.; Davidovits, P.; Worsnop, D.R.; Zahniser, M.S.; Kolb, C.E. Temperature dependence of the uptake coefficients of HNO_3, HCl and N_2O_5 by water droplets. *J. Phys. Chem.* **1990**, *94*, 3265–3269. [CrossRef]

19.   DeMore, W.B.; Sander, S.P.; Golden, D.M.; Hampson, R.F.; Kurylo, M.J.; Howard, C.J.; Ravishankara, A.R.; Kolb, C.E.; Molina, M.J. *Chemical Kinetics and Photochemical Data for Use in Stratospheric Modeling, Evaluation Number 12*; JPL Publication 97-4; Jet Propulsion Laboratory, National Aeronautics and Space Administration: Pasadena, CA, USA, 1997; 266p.

20.   Li, K.; Jacob, D.J.; Liao, H.; Shen, L.; Zhang, Q.; Bates, K.H. Anthropogenic drivers of 2013–2017 trends in summer surface ozone in China. *Proc. Nat. Acad. Sci. USA* **2019**, *116*, 422–427. [CrossRef] [PubMed]

21.   Department for Environment Food and Rural Affairs Air Quality Strategy: Framework for Local Authority Delivery. 2023. Available online: https://assets.publishing.service.gov.uk/media/64e8963d635870000d1dbf9d/Air_Quality_Strategy_Web.pdf (accessed on 15 May 2024).

22.   Department for Environment Food and Rural Affairs National Statistics. Particulate Matter (PM_{10}/$PM_{2.5}$). Available online: https://www.gov.uk/government/statistics/air-quality-statistics/concentrations-of-particulate-matter-pm10-and-pm25 (accessed on 15 May 2024).

23.   Air Quality Expert Group. Ozone in the UK—Recent Trends and Future Projections. 2021. Available online: https://uk-air.defra.gov.uk/assets/documents/reports/cat09/2112200932_Ozone_in_the_UK_Recent_Trends_and_Future_Projections.pdf (accessed on 15 May 2024).

24.   Holland, R.; Khan, M.A.H.; Derwent, R.G.; Lynch, J.; Ahmed, F.; Grace, S.; Bacak, A.; Shallcross, D.E. Gas-phase kinetics, POCPs and an investigation of the contributions of VOCs to urban ozone production in the UK. *Int. J. Chem. Kinet.* **2023**, *55*, 350–364. [CrossRef]

25.   Diaz, F.M.R.; Khan, M.A.H.; Shallcross, B.M.A.; Shallcross, E.D.G.; Vogt, U.; Shallcross, D.E. Ozone trends in the United Kingdom over the last 30 years. *Atmosphere* **2020**, *11*, 534. [CrossRef]

26. Department for Environment Food & Rural Affairs National Air Quality Data Archive. UK Air Information Resource. Available online: https://uk-air.defra.gov.uk/data/data_selector_service#mid (accessed on 15 May 2024).

27. Department for Environment Food & Rural Affairs Automatic Urban and Rural Network (AURN). Available online: https://uk-air.defra.gov.uk/networks/network-info?view=aurn (accessed on 15 May 2024).

28. Department for Environment Food & Rural Affairs. "Particulate Matter (PM$_{2.5}$ Targets) in the Environment Act: Monitoring Assessment Methods. Available online: https://uk-air.defra.gov.uk/networks/monitoring-methods?view=PM-Environment-Act-MonitoringMethods (accessed on 15 May 2024).

29. Department for Environment Food & Rural Affairs. The Air Quality Data Validation and Ratification Process. 2017. Available online: https://uk-air.defra.gov.uk/assets/documents/Data_Validation_and_Ratification_Process_Apr_2017.pdf (accessed on 15 May 2024).

30. Department for Environment Food & Rural Affairs. UK AIR Glossary. Available online: https://uk-air.defra.gov.uk/air-pollution/glossary (accessed on 15 May 2024).

31. Department for Environment Food & Rural Affairs. Automatic Hydrocarbon Network. Available online: https://uk-air.defra.gov.uk/networks/network-info?view=hc (accessed on 15 May 2024).

32. Department for Environment Food & Rural Affairs. Site Information for London Marylebone Road(UKA00315). Available online: https://uk-air.defra.gov.uk/networks/site-info?uka_id=UKA00315&search=View+Site+Information&action=site&provider=archive (accessed on 15 May 2024).

33. Wood, C.R.; ApSimon, H.; Arnold, S.; Balogun, A.A.; Barlow, J.F.; Belcher, S.E.; Britter, R.E.; Cheng, H.; Colvile, R.N.; Dobre, A.; et al. Dispersion experiments in central London: The 2007 DAPPLE project. *Bull. Am. Meteorol. Soc.* **2009**, *90*, 955–969. [CrossRef]

34. Martin, D.; Price, C.S.; Nickless, G.; Britter, R.E.; Londou, A.-N.; Neophytou, M.K.; Cheng, H.; Robins, A.G.; Dobre, A.; Belcher, S.E.; et al. Urban tracer dispersion experiments in London (DAPPLE) 2003: Field studies and comparisons with empirical prediction. *Atmos. Sci. Lett.* **2010**, *11*, 241–248. [CrossRef]

35. Balogun, A.; Tomlin, A.; Wood, C.; Barlow, J.; Belcher, S.; Smalley, R.; Lingard, J.; Arnold, S.; Dobre, A.; Robins, A.; et al. In-street wind direction variability in the vicinity of a busy intersection in Central London I. *Bound. Layer Meteorol.* **2010**, *136*, 489–513. [CrossRef]

36. Martin, D.; Price, C.S.; Nickless, G.; Britter, R.E.; Londou, A.-N.; Neophytou, M.K.; Cheng, H.; Robins, A.G.; Dobre, A.; Belcher, S.E.; et al. Urban tracer dispersion experiments during the second DAPPLE field campaign in London 2004. *Atmos. Environ.* **2010**, *44*, 3043–3052. [CrossRef]

37. Zhang, C.; Stevenson, D. Characteristic changes of ozone and its precursors in London during COVID-19 lockdown and the ozone surge season analysis. *Atmos. Environ.* **2022**, *273*, 118980. [CrossRef] [PubMed]

38. Kalisa, E.; Fadlallah, S.; Amani, M.; Nahayo, L.; Habiyaremye, G. Temperature and air pollution relationship during heatwaves in Birmingham, UK. *Sustain. Cities Soc.* **2018**, *43*, 111–120. [CrossRef]

39. Department for Environment Food & Rural Affairs. Site Information for Birmingham A4540 Roadside(UKA00626). Available online: https://uk-air.defra.gov.uk/networks/site-info?uka_id=UKA00626&search=View+Site+Information&action=site&provider=archive (accessed on 15 May 2024).

40. Garrido-Perez, J.M.; Ordóñez, C.; García-Herrera, R.; Schnell, J.L. The differing impact of air stagnation on summer ozone across Europe. *Atmos. Environ.* **2019**, *219*, 117062. [CrossRef]

41. Wang, T.; Xue, L.; Brimblecombe, P.; Lam, Y.F.; Li, L.; Zhang, L. Ozone pollution in China: A review of concentrations, meteorological influences, chemical precursors, and effects. *Sci. Total Environ.* **2017**, *575*, 1582–1596. [CrossRef] [PubMed]

42. Wakeling, D.; Passant, N.R.; Murrells, T.P.; Pang, Y.; Thistlethwaite, G.; Walker, C.; Brown, P.; del Vento, S.; Hunter, R.; Wiltshire, J.; et al. *UK Informative Inventory Report (1990 to 2015)*; DEFRA: London, UK, 2017; pp. 67–76.

43. Air Quality Expert Group. Fine Particulate Matter (PM$_{2.5}$) in the United Kingdom. 2012. Available online: https://uk-air.defra.gov.uk/assets/documents/reports/cat11/1212141150_AQEG_Fine_Particulate_Matter_in_the_UK.pdf (accessed on 15 May 2024).

44. Holland, R.; Seifert, K.; Saboya, E.; Khan, M.A.H.; Derwent, R.G.; Shallcross, D.E. Elucidating the effects of COVID-19 lockdowns in the UK on the O$_3$-NO$_x$-VOC relationship. *Atmosphere* **2024**, *15*, 607. [CrossRef]

45. Strong, J.; Whyatt, J.D.; Metcalfe, S.E.; Derwent, R.G.; Hewitt, C.N. Investigating the impacts of anthropogenic and biogenic VOC emissions and elevated temperatures during the 2003 ozone episode in the UK. *Atmos. Environ.* **2013**, *74*, 393–401. [CrossRef]

46. Harrison, R.M. Airborne particulate matter. *Philos. Trans. R. Soc. A* **2020**, *378*, 20190319. [CrossRef]

47. Vieno, M.; Heal, M.R.; Williams, M.; Carnell, E.; Nemitz, E.; Stedman, J.; Reis, S. The sensitivities of emissions reductions for the mitigation of UK PM$_{2.5}$. *Atmos. Chem. Phys.* **2016**, *16*, 265–276. [CrossRef]

48. Shao, M.; Wang, W.; Yuan, B.; Parrish, D.D.; Li, X.; Lu, K.; Wu, L.; Wang, X.; Mo, Z.; Yang, S. Quantifying the role of PM$_{2.5}$ dropping in variations of ground-level ozone: Inter-comparison between Beijing and Los Angeles. *Sci. Total Environ.* **2021**, *788*, 147712. [CrossRef] [PubMed]

49. Wang, N.; Lyu, X.; Deng, X.; Huang, X.; Jiang, F.; Ding, A. Aggravating O$_3$ pollution due to NO$_x$ emission control in eastern China. *Sci. Total Environ.* **2019**, *677*, 732–744. [CrossRef] [PubMed]

50. Sicard, P.; Paoletti, E.; Agathokleous, E.; Araminienè, V.; Proietti, C.; Coulibaly, F.; De Marco, A. Ozone weekend effect in cities: Deep insights for urban air pollution control. *Environ. Res.* **2020**, *191*, 110193. [CrossRef] [PubMed]

51. Amann, M.; Derwent, D.; Forsberg, B.; Hänninen, O.; Hurley, F.; Krzyzanowski, M.; de Leeuw, F.; Liu, S.J.; Mandin, C.; Schneider, J.; et al. *Health Risks of Ozone from Long-Range Transboundary Air Pollution*; World Health Organization (WHO) Regional Office for Europe: Copenhagen, Denmark, 2008.

52. Lewis, A.C.; Hopkins, J.R.; Carslaw, D.C.; Hamilton, J.F.; Nelson, B.S.; Stewart, G.; Dernie, J.; Passant, N.; Murrells, T. An increasing role for solvent emissions and implications for future measurements of volatile organic compounds. *Philos. Trans. R. Soc. A* **2020**, *378*, 20190328. [CrossRef] [PubMed]

53. Laxen, D.; Moorcroft, S.; Marner, B.; Laxen, K.; Boulter, P.; Barlow, T.; Harrison, R.; Heal, M. PM$_{2.5}$ in the UK, Report for *Scotland & Northern Ireland Forum for Environmnetal Research* (SNIFFER), Edinburgh. December 2010. Available online: https://www.aqconsultants.co.uk/CMSPages/GetFile.aspx?guid=eb3cd7b4-b297-46c5-a382-58113c04a105 (accessed on 16 June 2024).

54. Taseiko, O.V.; Mikhailuta, S.V.; Pitt, A.; Lezhenin, A.A.; Zakharov, Y.V. Air pollution dispersion within urban street canyons. *Atmos. Environ.* **2009**, *43*, 245–252. [CrossRef]

55. Tudor, C. Ozone pollution in London and Edinburgh; spatiotemporal characteristics, trends, transport and the impact of COVID-19 control measures. *Heliyon* **2022**, *8*, e11384. [CrossRef]

56. Papadogeorgou, G.; Kioumourtzoglou, M.-A.; Braun, D.; Zanobetti, A. Low levels of air pollution and health: Effect estimates, methodological challenges and future directions. *Curr. Environ. Health Rep.* **2019**, *6*, 105–115. [CrossRef]